Large displacement modeling for dynamic failure of concrete structure

Arnaud Delaplace, Adnan Ibrahimbegovic
LMT, ENS Cachan, 61, avenue du Président Wilson, 94235 Cachan, France.

ABSTRACT: rupture of reinforced concrete structures is often due to strain localisation in particular areas where microcracks nucleate to a macrocrack that propagates until complete failure. By taking into account material heterogeneity, a discrete model gives a fine description of the crack properties (path, roughness...). We present in this work a particular discrete model that manages the large displacements encountered near the crack tip. Different examples illustrate the model performance.

1 INTRODUCTION

Describing the failure of concrete structures requires a clear representation of the mechanical response (force vs. displacement for instance) as well as a good description of crack properties. This last goal can be achieved by taking into account the heterogeneity of the material, which is a typical feature of discrete models.

Our development is based on such a discrete model, where material is described as an assembly of particles (see [2], [8], [1] for instance). Between each neighboring particles, brittle elastic links are used to model initial cohesion forces. During the elastic range, the model is strictly equivalent to lattice models ([7], [9], [10]). During the nonlinear behavior, contact forces are introduced if unlinked particles overlap each other. Note that if all beams are broken, a non-cohesive material behavior is obtained. These kind of models are known to be relevant to describe crack propagation during the failure of a structure. The proposed discrete model is enriched in order to take into account large displacement, by using a particular nonlinear beam model of Reissner, which allowing a representation of all the fracture mechanisms. Because a large number of particles is used for each computation, we focus on the numerical implementation of the beam, where the computational time has been optimized by obtaining the tangent operator.

The extension to dynamic loading is proposed, with a particular attention to physical results in terms of dissipation: nonlinear behavior is known to give non physical generation of energy with some time integration schemes. After a comparison of classical schemes (explicit scheme, Newmark family schemes, HHT), we propose the use of a particular scheme that ensures energy dissipation even with non linear behavior.

2 DISCRETE MODEL

The proposed approach is based on a description of material heterogeneity by an assembly of rigid voronoi cells (Figure 1). These cells are connected initially by flexible links which ensure the elastic behavior. The majority of discrete models use either springs or linear beams (Euler-Bernoulli or Timochenko) for these links. This choice is valid for a wide range of problems, but we would like to emphasize different cases where large displacement occurs and such beams can not represent the right behavior: near a crack tip, large rotations can occur particularly for reinforced concrete structure where steel bars allow plastic deformation. Beam scabbing is an other example where linked cells can fall out the main structure, and be subject to large displacement. We propose here to use beams which can account for such large displacements. The main properties of the beams are presented in the next part.

Large displacement beams The initial configuration of the beam is placed along the axis of the reference frame $(\mathbf{e}_1, \mathbf{e}_2)$. A point at the typical section of the beam initially placed at (x, y) in the deformed configuration can be represented by its position vector $\boldsymbol{\phi}$:

$$\boldsymbol{\phi} = (x + u)\mathbf{e}_1 + v\mathbf{e}_2 + y\mathbf{t}_2 \qquad (1)$$

where u and v are the displacement components and $\mathbf{t}_2$ is a unit vector indicating the new direc-
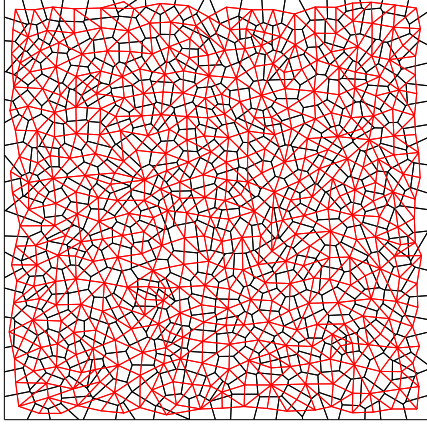
Figure 1: Cells assembly describing a square. Thin lines represent links.

tion of the cross section (not necessarily perpendicular to the beam neutral axis). According to Reissner's kinematic hypothesis the cross-section remains non-deformable, so that vector $\mathbf{t}_2$ can be obtained simply by a rotation of the base vector $\mathbf{e}_2$.

$$\mathbf{t}_2 = \mathbf{\Lambda}\mathbf{e}_2; \quad \mathbf{\Lambda} = \begin{bmatrix} \cos\psi & -\sin\psi \\ \sin\psi & \cos\psi \end{bmatrix} \quad (2)$$

where ψ is the rotation angle. The corresponding deformation measure of Biot can the be provided for the beam as

$$H_{11}(x,y) = \Sigma(x) - yK(x)$$

$$H_{21}(x,y) = \Gamma(x) \quad (3)$$

where

$$\Sigma(x) = \mathbf{t_1} \cdot \boldsymbol{\phi}' - \mathbf{e_1} \cdot \mathbf{e_1}$$

$$K(x) = \mathbf{t_2}' \cdot \mathbf{t_1}$$

$$\Gamma(x) = \mathbf{t_2} \cdot \boldsymbol{\phi}' - \mathbf{e_2} \cdot \mathbf{e_1}$$

Discretisation of the last equations gives the following relations for two nodes 1 and 2 if we assume that each strain component remains constant along the beam:

$$\Sigma = \cos\left(\frac{\psi_1 + \psi_2}{2}\right)\left(1 + \frac{u_2 - u_1}{l}\right)$$

$$+ \sin\left(\frac{\psi_1 + \psi_2}{2}\right)\left(\frac{v_2 - v_1}{l}\right) - 1$$

$$\Gamma = -\sin\left(\frac{\psi_1 + \psi_2}{2}\right)\left(1 + \frac{u_2 - u_1}{l}\right) \quad (4)$$

$$+ \cos\left(\frac{\psi_1 + \psi_2}{2}\right)\left(\frac{v_2 - v_1}{l}\right)$$

$$K = \frac{\psi_2 - \psi_1}{2}$$

In the elastic domain one can easily obtain the associated Biot stress through Hook's law by

$$T_{11}(x,y) = E(x,y)H_{11}(x,y)$$

$$T_{21}(x,y) = G(x,y)H_{21}(x,y) \quad (5)$$

where E and G are, respectively, Young's and shear moduli. The elastic constitutive model in (5) above applies only before reaching the fracture limit. Finally, we can obtain (see [5]) the relative axial/shear deformation between two neighboring cells i and j with

$$\varepsilon_{ij} = \left(\frac{\Delta s}{l_{ij}}\right) = \left((1 + \Sigma)^2 + \Gamma^2\right)^{1/2} \quad (6)$$

and, in the same manner, we can obtain the relative rotation

$$K = \frac{\psi_2 - \psi_1}{l_{ij}} \quad (7)$$

Inelastic behavior The nonlinear behavior of model is obtained by introducing a breaking threshold for each beam. It leads to a perfectly brittle-elastic behavior at microscale, according to the local behavior of a heterogeneous brittle material. The fracture criterion [3] for any pair of neighboring particles i and j is:

$$P_{ij} = \left(\frac{\varepsilon_{ij}}{\varepsilon_{ij}^{cr}}\right)^2 + \left(\frac{|\psi_i - \psi_j|}{\psi_{ij}^{cr}}\right) \geq 1 \quad (8)$$

where the fracture limit values ε_{ij}^{cr} and ψ_{ij}^{cr} are considered to be random variables with Gaussian distribution. ε_{ij}^{cr} corresponds to rupture of the beam in tension mode, ψ_{ij}^{cr} corresponds to rupture of the beam in bending mode. When the failure criterion is reached, the beam ij is broken and both particles i and j are no more linked. The heterogeneous microstructure can thus be represented in a simple way by varying the fracture limit values of particular beam links.

Numerical Example We present here the classical example of the beam scabbing. The beam is loaded by an impulse-type loading at the upper face, with three-point bending test boundary conditions (Figure 2).
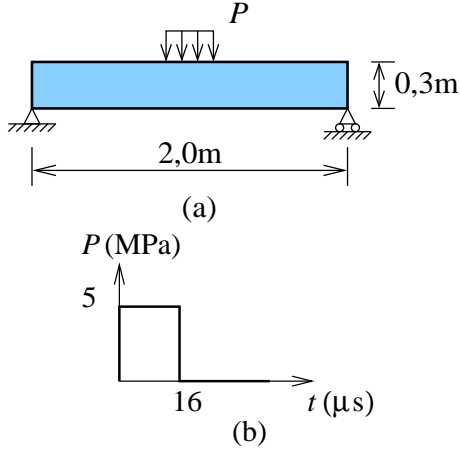
Figure 2: Boundary conditions of the beam scabbing test.

As mentioned before, this test is discriminant for the model because large deformations occur for cells falling out at the bottom face of the beam. Crack patterns are shown at different times on Figure 3. Large displacements are clearly visible in the two last shots.
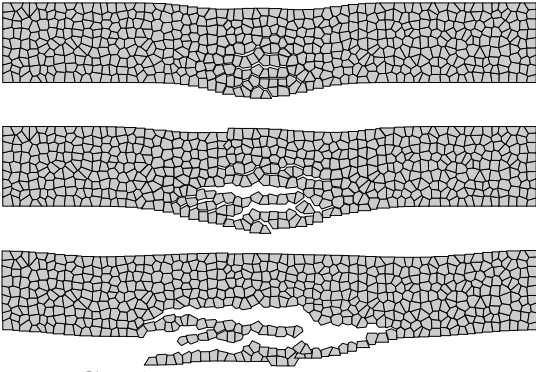

Figure 3: Crack patterns at $t = 350\mu$s, $t = 500\mu$s and $t = 1000\mu$s.

3   TIME INTEGRATION SCHEME

One of the main difficulty encountered with such a model is the effect of brittle failure of the bonds in a dynamic analysis. It leads to high frequency vibrations without physical meaning (Figure 4).

We propose in this part to compare different schemes and analyze their performance (see [11] for an overview of time stepping schemes). We use the same boundary conditions as shown on Figure 4, but the load is chosen such to keep an elastic behavior. High frequencies will be introduced through an impulse loading (Figure 5).

The impulse created by the instantaneous relaxation of loading is equivalent to the impulse created by the failure of one link. For $t > 2$ ms, the specimen oscillates vertically at low frequencies in free vibration phase. These low frequencies have a physical interpretation and should not be damped.
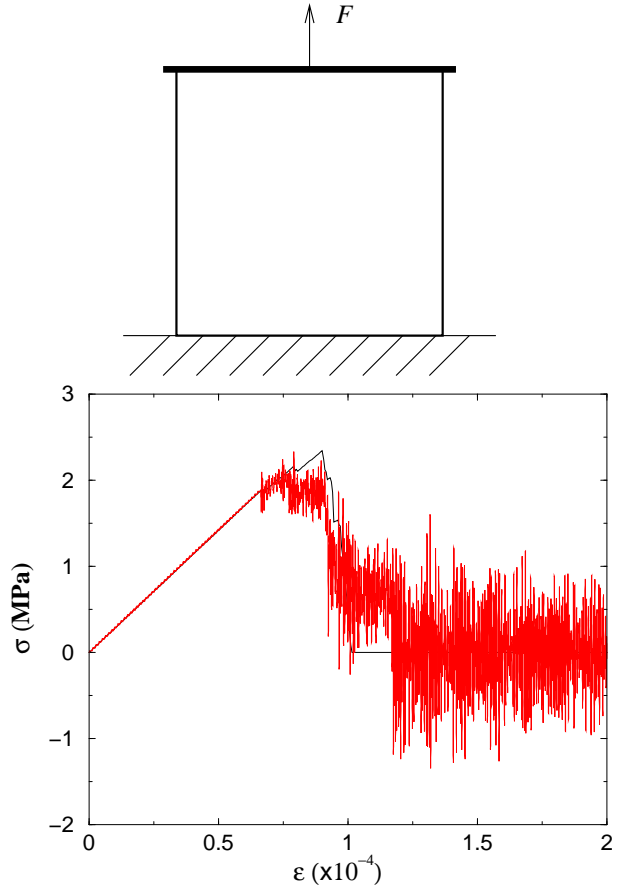

Figure 4: Response of dynamic tension test on a square (0,1 m×0,1 m) without numerical damping.
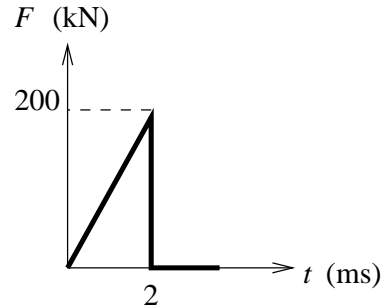

Figure 5: Elastic load for dynamic test.

On the other hand, high frequencies created by the force impulse have to be damped. This goal should be reached by the time integration scheme.

For a typical time step Δt, we have to compute displacement $\mathbf{d}_{t+\Delta t}$, velocity $\mathbf{v}_{t+\Delta t}$ and acceleration vector $\mathbf{d}_{a+\Delta t}$, containing the motion components for particle centers, which satisfy the equations of motion at time $t + \Delta t$

$$\mathbf{M}\mathbf{a}_{t+\Delta t} + \mathbf{C}\mathbf{v}_{t+\Delta t} + \mathbf{F}^{int}(\mathbf{d}_{t+\Delta t}) = \mathbf{F}^{ext}_{t+\Delta t} \quad (9)$$

Explicit scheme   For high-rate loading, the most employed scheme is an explicit one based on the central different scheme. The main advantage of this scheme is that for a diagonal form of the mass matrix and a constant damping, the compu-

tational cost is very low. The main draw-back is its conditional stability. However, this scheme is employed for fast load like beam scabbing test, where high or low frequencies do not need to be damped.

Implicit scheme The unconditional stability is obtained through an implicit scheme. The most employed one is time integration by trapezoidal rule (or Newmark implicit scheme). In that case, the displacement and velocity approximation are

$$\mathbf{d}_{t+\Delta t} = \mathbf{d}_t + \Delta t \mathbf{v}_t + (\Delta t)^2 \left((\frac{1}{2} - \beta)\mathbf{a}_t + \beta \mathbf{a}_{t+\Delta t} \right)$$

$$\mathbf{v}_{t+\Delta t} = \mathbf{v}_t + \Delta t \left((1 - \gamma)\mathbf{a}_t + \gamma \mathbf{a}_{t+\Delta t} \right) \quad (10)$$

where $\beta = 1/4$ and $\gamma = 1/2$ are the most appropriate values of the Newmark parameters corresponding to trapezoidal rule. Linearized form of this system to be used in the Newton iterative procedure is written as:

$$\left(\frac{1}{\beta(\Delta t)^2}\mathbf{M} + \frac{\gamma}{\beta \Delta t}\mathbf{C} + \mathbf{K}(\mathbf{d}_t) \right)\Delta\mathbf{d} =$$

$$\mathbf{F}^{ext}_{t+\Delta t} - \mathbf{K}(\mathbf{d}_t)\mathbf{d}_t$$

$$+\mathbf{C}\left((\frac{\gamma}{\beta} - 1)\mathbf{v}_t + \Delta t(\frac{\gamma}{2\beta} - 1)\mathbf{a}_t \right)$$

$$+\mathbf{M}\left(\frac{1}{\beta \Delta t}\mathbf{v}_t + (\frac{1}{2\beta} - 1)\mathbf{a}_t \right) \quad (11)$$

No damping is introduced with this scheme. One can introduce numerical dissipation by choosing higher values of the Newmark parameter, but the scheme is no longer of second accuracy.

HHT scheme A derived scheme of the Newmark one is the HHT-α scheme, which has been developed in order to damp high frequencies [4]. The idea is to change equation of motion to

$$\mathbf{M}\mathbf{a}_{t+\Delta t} + (1 + \alpha)\mathbf{C}\mathbf{v}_{t+\Delta t} - \alpha\mathbf{C}\mathbf{v}_t$$

$$+(1 + \alpha)\mathbf{K}(\mathbf{d}_{t+\Delta t})\mathbf{d}_{t+\Delta t} - \alpha\mathbf{K}(\mathbf{d}_t)\mathbf{d}_t =$$

$$(1 + \alpha)\mathbf{F}^{ext}_{t+\Delta t} - \alpha\mathbf{F}^{ext}_t \quad (12)$$

where α is a parameter chosen as $\alpha \in [-1/3, 0]$ whereas the other parameters are $\beta = \frac{1}{4}(1 - \alpha)^2$ and $\gamma = \frac{1}{2} - \alpha$.

Linearized form of this system to be used in the Newton iterative procedure is written as:

$$\left(\frac{1}{\beta(\Delta t)^2}\mathbf{M} + (1 + \alpha)\left(\frac{\gamma}{\beta \Delta t}\mathbf{C} + \mathbf{K}(\mathbf{d}_t) \right) \right)\Delta\mathbf{d} =$$

$$(1 + \alpha)\mathbf{F}^{ext}_{t+\Delta t} - \alpha\mathbf{F}^{ext}_t - \mathbf{K}(\mathbf{d}_t)\mathbf{d}_t + \alpha\mathbf{C}\mathbf{v}_t$$

$$+(1 + \alpha)\mathbf{C}\left((\frac{\gamma}{\beta} - 1)\mathbf{v}_t + \Delta t(\frac{\gamma}{2\beta} - 1)\mathbf{a}_t \right)$$

$$+\mathbf{M}\left(\frac{1}{\beta \Delta t}\mathbf{v}_t + (\frac{1}{2\beta} - 1)\mathbf{a}_t \right) \quad (13)$$

This scheme is probably the best one for our kind of model with linear beams. But when nonlinear beams are used, this scheme can lead to numerical problem like generation of energy rather its dissipation. The last proposed scheme avoid this kind of non physical behavior.

Time integration with energy decaying scheme This last scheme keeps dissipation of high frequencies, and ensure the energy decay for a non-linear behavior (see [6] for application to nonlinear beams). The equation of motion are written at time $t + \Delta t/2$:

$$\mathbf{M}\mathbf{a}_{t+\frac{\Delta t}{2}} + \mathbf{C}\mathbf{v}_{t+\frac{\Delta t}{2}} + \mathbf{K}(\mathbf{d}_{t+\frac{\Delta t}{2}})\mathbf{d}_{t+\frac{\Delta t}{2}} =$$

$$\mathbf{F}^{ext}_{t+\frac{\Delta t}{2}} \quad (14)$$

Energy decaying is obtained by introducing the dissipation when computing the internal forces and the inertia terms, as

$$\mathbf{K}(\mathbf{d}_{t+\frac{\Delta t}{2}})\mathbf{d}_{t+\frac{\Delta t}{2}} = \frac{1}{2}(\mathbf{K}(\mathbf{d}_{t+\Delta t})\mathbf{d}_{t+\Delta t} + \mathbf{K}(\mathbf{d}_t)\mathbf{d}_t) +$$

$$\alpha_1(\mathbf{K}(\mathbf{d}_{t+\Delta t})\mathbf{d}_{t+\Delta t} - \mathbf{K}(\mathbf{d}_t)\mathbf{d}_t)$$

and the inertia terms and velocity are changed to :

$$\mathbf{d}_{t+\Delta t} = \mathbf{d}_t + \frac{\Delta t}{2}(\mathbf{v}_{t+\Delta t} + \mathbf{v}_t)$$

$$+\alpha_2\Delta t(\mathbf{v}_{t+\Delta t} - \mathbf{v}_t)$$

where α_1 and α_2 are the two parameters that control the dissipation. Linearized form of the system is:

$$\left(\frac{2}{(1 + 2\alpha_2)(\Delta t)^2}\mathbf{M} + \frac{1}{(1 + 2\alpha_2)\Delta t}\mathbf{C} \right.$$

$$\left. +(\frac{1}{2} + \alpha_1)\mathbf{K}(\mathbf{d}_t) \right)\Delta\mathbf{d} =$$

$$\frac{1}{2}\mathbf{F}^{ext}_{t+\Delta t} + \frac{1}{2}\mathbf{F}^{ext}_t - \mathbf{K}(\mathbf{d}_t)\mathbf{d}_t$$

$$-\frac{2\alpha_2}{1 + 2\alpha_2}\mathbf{C}\mathbf{v}_t + \mathbf{M}\left(\frac{2}{(1 + 2\alpha_2)\Delta t}\mathbf{v}_t \right) \quad (15)$$

4

At $\alpha_1 = \alpha_2 = 0$, no dissipation is introduced. Large values ($\alpha_1 = \alpha_2 > 0.5$) give undesirable dissipation of low frequencies. For our numerical computations, $\alpha_1 = \alpha_2 = 0.05$ give good results with dissipation of high frequencies in less than ten low-frequency oscillations ($\Delta t = 10^{-6}$ s).

Numerical results obtained with this scheme are shown on Figures 6 and 7. Figure 6 shows the vertical and horizontal displacement of a particle located at the top of the specimen. The vertical displacement (dashed line) show low frequencies corresponding to free oscillations of the specimen. On the other hand, horizontal displacement (continuous line) is the juxtaposition of high and low frequencies. As expected, after few oscillations, just high frequencies are damped. Figure 7 shows the evolution and the dissipation of energy during the loading.
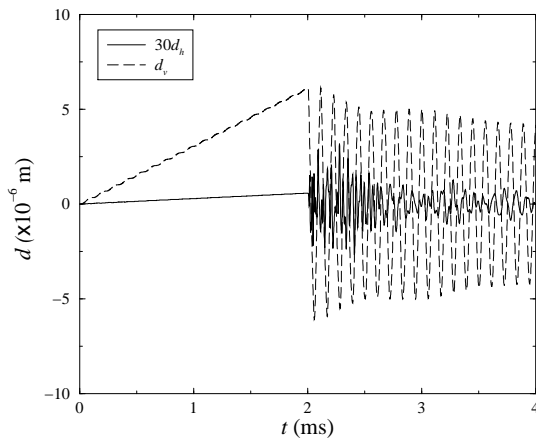

Figure 6: Horizontal and vertical displacements of a particle at the top of the specimen.
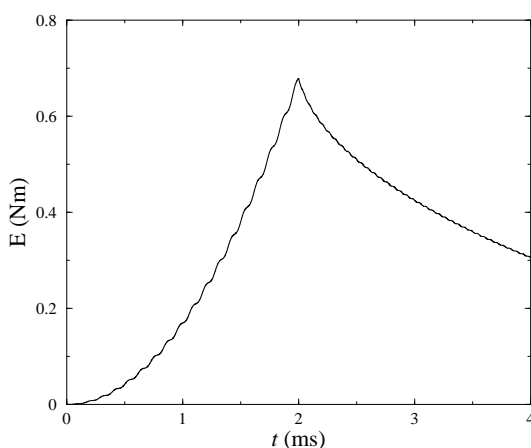

Figure 7: Energy evolution during the loading.

4 CONCLUSIONS

A discrete model based on a voronoi cell description of the material is proposed. Cohesive forces are represented by nonlinear beams, allowing to take into account large displacements of the cells. Static and dynamic analysis are proposed and a particular attention is given to time integration schemes. We have tested explicit schemes for high rate loading, as well as implicit schemes for low rate loading. The chosen dynamic scheme has to damp non physical high frequencies due to link ruptures, and we proposed the use of a particular scheme which damps these frequencies and guarantees the dissipation of energy, either in nonlinear case.

REFERENCES

[1] J.E. Bolander and S. Saito. Fracture analysis using spring networks with random geometry. *Engineering Fracture Mechanics*, 61:569–591, 1998.

[2] P.A. Cundall and O.D.L. Strack. A discrete numerical model for granular assemblies. *Géotechnique*, 29:47–65, 1979.

[3] H. J. Herrmann and Stéphane Roux. *Statistical models for the fracture of disordered media.* Elsevier Science Publishers, Amsterdam, 1990.

[4] H.M. Hilbert, T.J.R. Hughes, and R.L. Taylor. Improved numerical dissipation for time integration algorithms in structural dynamics. *Int. J. Earthq. Eng. Struct. Dynam.*, 5:283–292, 1977.

[5] A. Ibrahimbegovic and A. Delaplace. Microscale and mesoscale discrete models for dynamic fracture of structures built of brittle material. *Comput. Struct.*, 81:1255–1265, 2003.

[6] A. Ibrahimbegovic and S. Mamouri. Energy conserving/decaying implicit time-stepping scheme for nonlinear dynamics of three-dimensional beams undergoing finite rotations. *Computer Methods in Applied Mechanics and Engineering*, 191:4241–4258, 2002.

[7] M. Jirasek and Z. P. Bazant. Macroscopic fracture characteristics of random particle systems. *International Journal of Fracture*, 69:201–228, 1995.

[8] F. Kun and H.J. Herrmann. A study of fragmentation processes using a discrete element method. *Comp. Meth. Appl. Mech. Eng.*, 7:3–18, 1996.

[9] E. Schlangen and E.J. Garboczi. Fracture simulations of concrete using lattice models: Computational aspects. *Eng. Fracture Mech.*, 57:319–332, 1997.

[10] J.G.M. Van Mier and M.R.A. Van Vliet. Influence of microstructure of concrete on size/scale effects in tensile fracture. *Eng. Fracture Mech.*, 70:2281–2306, 2003.

[11] O.C. Zienkiewicz and R.L. Taylor. *The finite element method, Vol. 1,2 and 3, 5th ed.* Butterworth, Heinemann, Oxford, 2000.